SCIENTIFIC REPORTS

OPEN

SUBJECT AREAS:
TWO-DIMENSIONAL MATERIALS
ELECTRONIC PROPERTIES AND MATERIALS
SURFACES, INTERFACES AND THIN FILMS

Received
12 February 2014

Accepted
28 March 2014

Published
22 April 2014

Correspondence and requests for materials should be addressed to A.A.S. (saranin@iacp.dvo.ru)

A Strategy to Create Spin-Split Metallic Bands on Silicon Using a Dense Alloy Layer

Dimitry V. Gruznev[1,2], Leonid V. Bondarenko[1,2], Andrey V. Matetskiy[1,2], Alexey A. Yakovlev[1], Alexandra Y. Tupchaya[1], Sergey V. Eremeev[3,4], Evgeniy V. Chulkov[4,5,6], Jyh-Pin Chou[7], Ching-Ming Wei[7], Ming-Yu Lai[7], Yuh-Lin Wang[7], Andrey V. Zotov[1,2,8] & Alexander A. Saranin[1,2]

[1]Institute of Automation and Control Processes FEB RAS, 690041 Vladivostok, Russia, [2]Far Eastern Federal University, School of Natural Sciences, 690950 Vladivostok, Russia, [3]Institute of Strength Physics and Materials Science, 634021 Tomsk, Russia, [4]Tomsk State University, 634050 Tomsk, Russia, [5]Donostia International Physics Center (DIPC), 20018 San Sebastían/Donostia, Basque Country, Spain, [6]Departamento de Física de Materiales UPV/EHU, CFM-MPC and Centro Mixto CSIC-UPV/EHU, 20080 San Sebastían/Donostia, Basque Country, Spain, [7]Institute of Atomic and Molecular Sciences, Academia Sinica, P.O. Box 23-166 Taipei, Taiwan, [8]Department of Electronics, Vladivostok State University of Economics and Service, 690600 Vladivostok, Russia.

To exploit Rashba effect in a 2D electron gas on silicon surface for spin transport, it is necessary to have surface reconstruction with spin-split metallic surface-state bands. However, metals with strong spin-orbit coupling (e.g., Bi, Tl, Sb, Pt) induce reconstructions on silicon with almost exclusively spin-split insulating bands. We propose a strategy to create spin-split metallic bands using a dense 2D alloy layer containing a metal with strong spin-orbit coupling and another metal to modify the surface reconstruction. Here we report two examples, i.e., alloying Bi/Si(111)$\sqrt{3}\times\sqrt{3}$ reconstruction with Na and Tl/Si(111)1 × 1 reconstruction with Pb. The strategy provides a new paradigm for creating metallic surface state bands with various spin textures on silicon and therefore enhances the possibility to integrate fascinating and promising capabilities of spintronics with current semiconductor technology.

The Rashba spin splitting[1,2] in the two-dimensional electron gas systems on semiconductors is considered to be the key concept for many promising spintronics applications. To combine Rashba-effect based spintronics with a silicon technology *metallic surface states* with *a strong spin-orbit coupling* on *a silicon* surface[3,4] are demanded. Unfortunately, the most of the metal/silicon systems with spin-split surface state bands (e.g., Bi/Si(111)$\sqrt{3}\times\sqrt{3}$ [5–7], Tl/Si(111)1 × 1 [8–10], Sb/Si(111)$\sqrt{3}\times\sqrt{3}$ [11] and Pt/Si(110)"6" × 5 [12]) are *semiconducting*. The only known exceptions are the Tl/Si(111)1 × 1 modified by adsorption of additional Tl[13] and Au/Si(111)$\sqrt{3}\times\sqrt{3}$ modified by adsorption of In, Tl, Cs or Na[4]. It is worth noting that in both cases adsorbates do not alter the basic atomic arrangement of the pristine surface and their effect resides just in eliminating or generating surface defects (as for Au/Si(111) and Tl/Si(111), respectively) and doping electrons to the available surface-state bands. In the present study, we propose a novel more universal strategy for tailoring the spin-split metallic surface states. The main concept resides in formation of the 2D alloy layers containing a metal with a strong spin-orbit coupling and another suitable metal to obtain dense reconstructions with spin-split *metallic* bands. Validity of the approach is demonstrated by the formation of the Bi-Na and Tl-Pb 2D alloys on Si(111) surface possessing the required properties.

Results

Figure 1 (left panel) summarizes the main structural and electronic properties of the pristine β−Bi/Si(111)$\sqrt{3}\times\sqrt{3}$ surface. It contains 1.0 ML (monolayer, 7.8 × 10^{14} cm^{-2}) of Bi arranged into the trimers centered at the T_4 sites on the bulk-truncated Si(111) surface[14]. The main features of its electronic structure are spin-split non-metallic bands, *S*1 (*S*1′) and *S*2 (*S*2′)[6]. Room-temperature (RT) deposition of 0.33 ML Na onto this surface results in the formation of the ordered Bi-Na alloy layer whose structural and electronic properties are shown in Figure 1 (right panel). Comparison of its atomic structure with that of the original β−Bi/Si(111)$\sqrt{3}\times\sqrt{3}$ surface demonstrates that the Bi trimers are preserved but they increase in size by ~8% (Bi-Bi bond length changes from 3.13 to 3.34 Å) and twisted by ±6.8°. The resultant arrangement of Bi atoms at the surface can be thought then as a

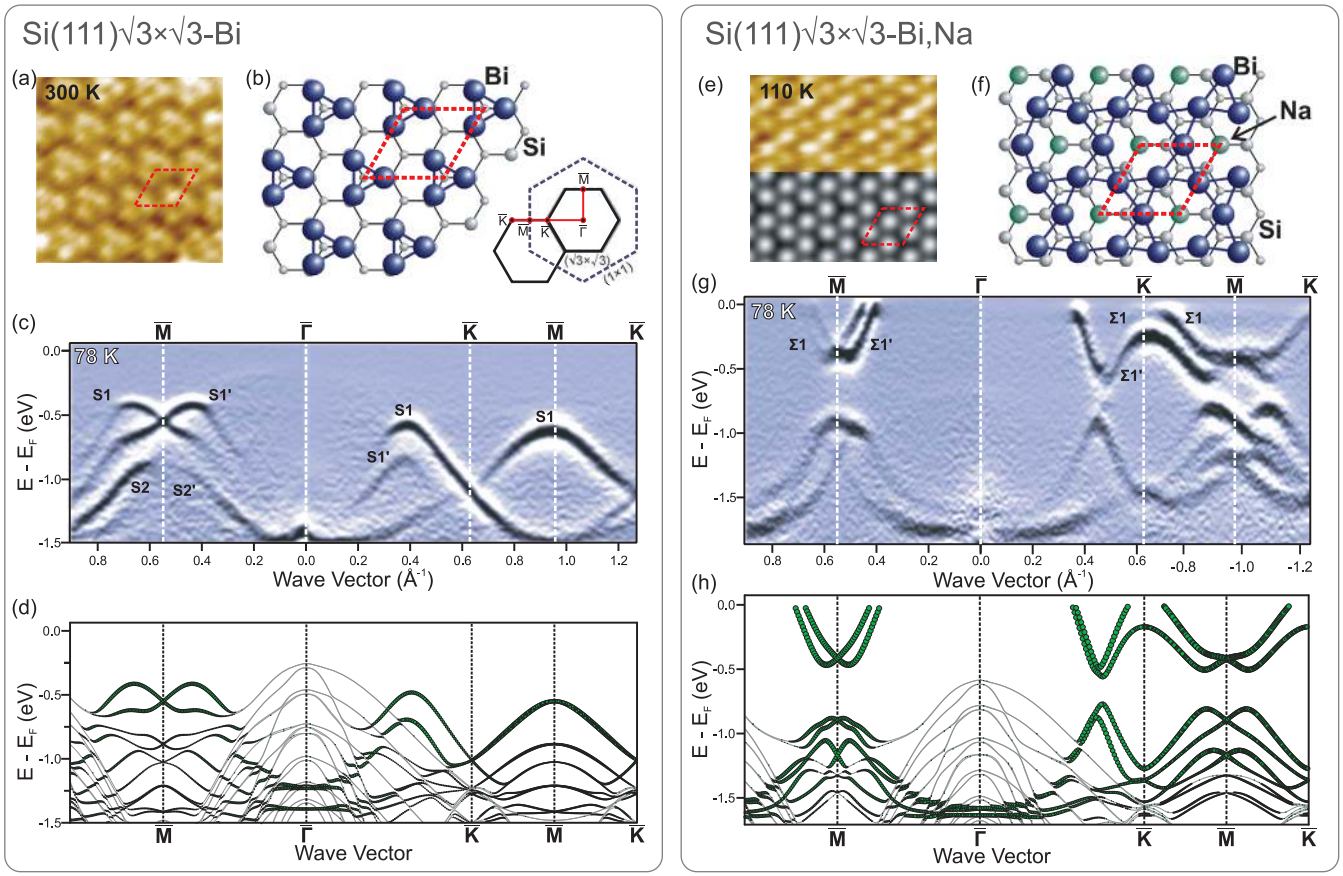

Figure 1 | Structural and electronic properties of the Bi/Si(111)$\sqrt{3}\times\sqrt{3}$ (left panel) and (Bi, Na)/Si(111)$\sqrt{3}\times\sqrt{3}$ (right panel). (a) and (e) 30 × 30 Å^2 STM images. Upper and lower halves in (e) present experimental and simulated empty-state (+0.3 V) STM images, respectively. (b) and (f) Structural models where Bi atoms are shown by violet circles, Na atoms by green circles, and Si atoms by gray circles. Positions of the outlined $\sqrt{3}\times\sqrt{3}$ unit cells in (e) and (f) correspond to each other. The inset in (b) shows a sketch of reciprocal space geometry with boundaries of the $\sqrt{3}\times\sqrt{3}$ and 1 × 1 SBZs given by solid black and dashed blue lines, respectively. (c) and (g) Experimental ARPES spectra and (d) and (h) calculated electronic band structures. In the calculated band structures, the size of green circles corresponds to the strength of the surface character summed over all orbitals at a particular $k_{||}$ value.

honeycomb network of the chained Bi trimers with Na atoms occupying the T_4 sites in the center of each honeycomb unit.

Changes in atomic structure of the surface cause modification of its electronic band structure as revealed by angle-resolved photoelectron spectroscopy (ARPES) measurements and density-functional theory (DFT) calculations (Figure 1g and h). We would like to remark that a perfect agreement between the calculated band structure and that determined in the experiment as well as coincidence of the experimental and simulated STM images can serve an indication of the proper (Bi, Na)/Si(111) structural model. The most essential feature in the Bi-Na alloy band structure is the appeared metallic spin-split surface-state band denoted by Σ1 (Σ1′).

Consider now the Pb-induced modification of the Tl/Si(111)1 × 1 surface. Figure 2 (left panel) presents the main structural and electronic properties of the pristine Tl/Si(111)1 × 1 reconstruction. It contains 1.0 ML of Tl atoms occupying every T_4 site on the bulk-truncated Si(111) surface[15–17]. The band structure of the Tl/Si(111)1 × 1 surface includes the insulating *S*1 surface-state band whose occurrence was proved before both experimentally[8,15] and theoretically[9,15]. Spin-splitting of this band has been concluded from the spin-resolved ARPES results[8] and from previous[9] and current theoretical calculations (Figure 2d) and is clearly resolved in the spin-unpolarized ARPES spectrum in Figure 2c. Additional feature can be noted, namely, the shallow metallic band *S*2 around the $\overline{K}$ point. It has recently been recognized that electron filling of this band is associated with extra Tl atoms on the Tl/Si(111)1 × 1 surface[13] in the form of specific surface defects[18].

Adding 0.33 ML of Pb to the Tl/Si(111)1 × 1 surface at RT produces a homogeneous Tl-Pb alloy having $\sqrt{3}\times\sqrt{3}$ periodicity. Its atomic arrangement (Figure 2f) looks qualitatively akin that of the Bi-Na alloy (Figure 1f), namely the first adsorbate, Bi or Tl, form the chained trimers arranged into a honeycomb network, while atoms of the second adsorbate, Na or Pb, occupy the centers of the honeycomb units. The difference is that Pb atom residence and Tl trimers centers in the Tl-Pb alloy are in the T_1 (on-top) sites while the positions of Na atoms and Bi trimers in the Bi-Na alloy are the T_4 sites. Both Bi-Na and Tl-Pb alloys are confined essentially in single atomic layers with Na being by ~0.62 Å higher than Bi and Pb by 0.37 Å higher than Tl.

Substantial structural changes due to Tl/Pb alloying, including, in particular, the change in the surface periodicity, 1 × 1 to $\sqrt{3}\times\sqrt{3}$, leads to changing the band structure. The most essential newly developed features are the two spin-split metallic surface-state bands (denoted by Σ1 (Σ1′) and Σ2 (Σ2′)) which are clearly seen in Figure 2g and h.

The calculated Fermi surfaces of the alloys reproduce nicely the contours observed experimentally (Figure 3). The main features of the alloy spin texture predicted by DFT calculations are also illustrated in Figure 3. The planar spin components show in-plane helicity, suggestive of a Rashba scenario. For momentum vectors along the $\overline{\Gamma}-\overline{K}$ directions, the spin is fully aligned in-plane and perpendicular to the momentum vector. The out-of-plane spin component undulates between positive and negative values along the contours according to the C_{3v} symmetry of the surfaces.

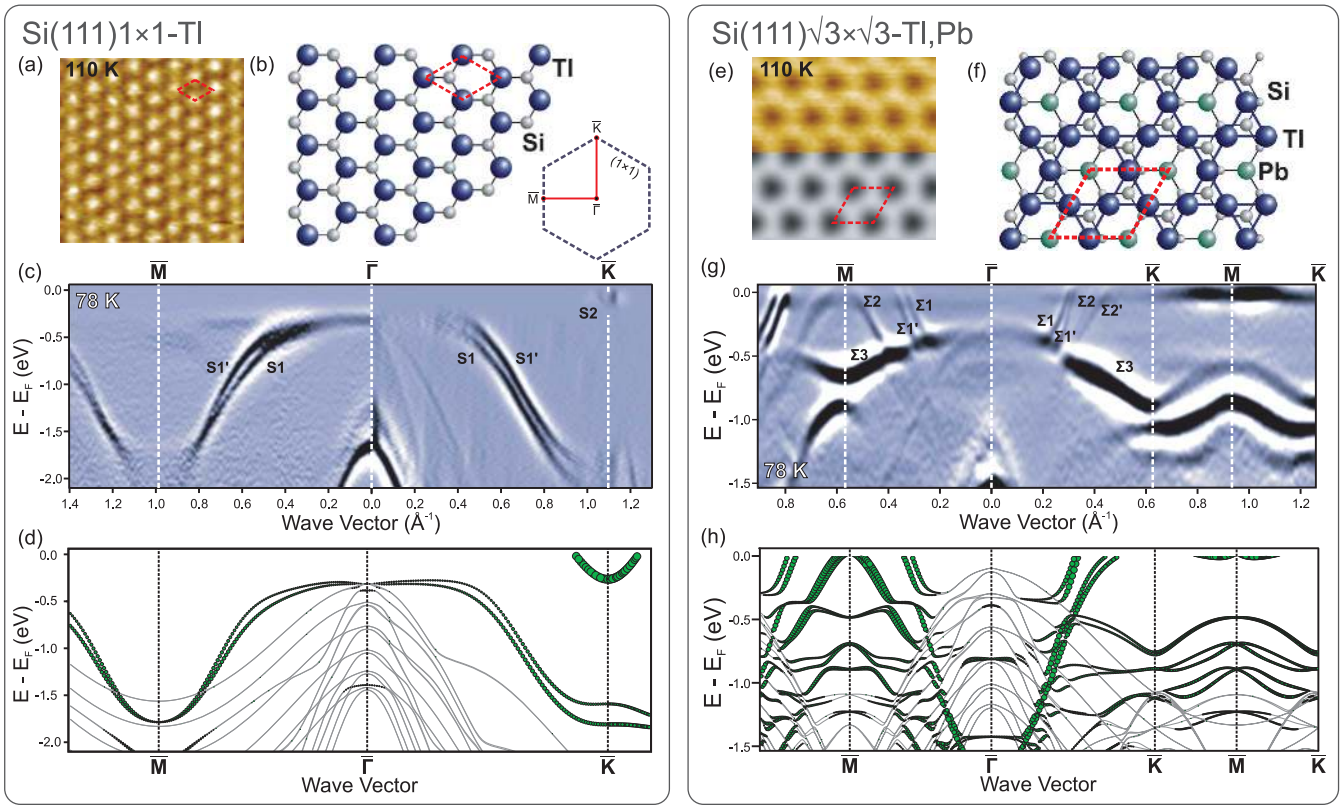

Figure 2 | Structural and electronic properties of the Tl/Si(111)1 × 1 (left panel) and (Tl, Pb)/Si(111)$\sqrt{3}\times\sqrt{3}$ (right panel). (a) and (e) 30 × 30 Å^2 empty-state (+0.4 V) STM images. Upper and lower halves in (e) present experimental and simulated empty-state (+0.4 V) STM images, respectively. (b) and (f) Structural models where Tl atoms are shown by violet circles, Pb atoms by green circles, and Si atoms by gray circles. Positions of the outlined $\sqrt{3}\times\sqrt{3}$ unit cells in (e) and (f) correspond to each other. (c) and (g) Experimental ARPES spectra and (d) and (h) calculated electronic band structures.

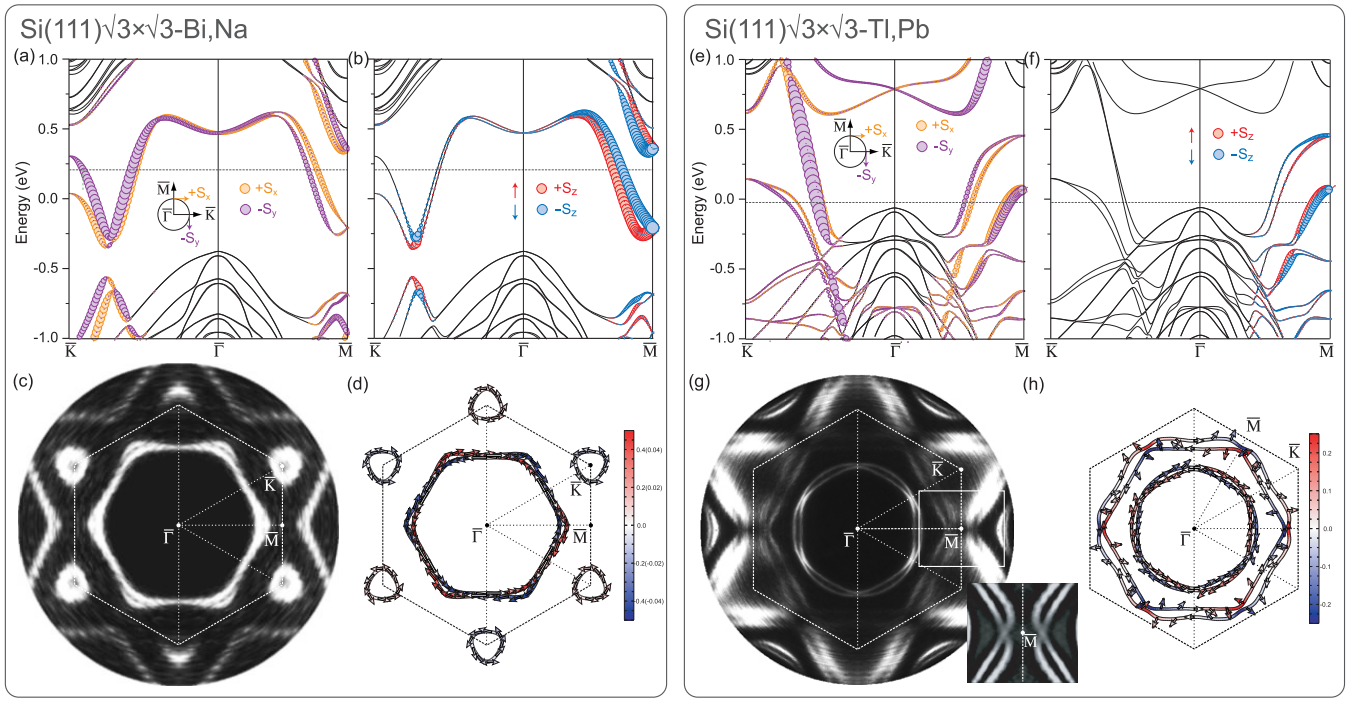

Figure 3 | Calculated band structure of the (Bi,Na)/Si(111)$\sqrt{3}\times\sqrt{3}$ (left panel) and (Tl,Pb)/Si(111)$\sqrt{3}\times\sqrt{3}$ (right panel) including spin-orbit coupling illustrating the (a, e) in-plane and (b, f) out-of-plane polarization components. (c, g) Experimental and (d, h) calculated Fermi contours. Inset in (g) shows the fine structure within the outlined area around the $\overline{M}$ point with a greater contrast. Arrows adjacent to the calculated contours and their length denote the in-plane spin component. The out-of-plane spin component is indicated by the colour with red and blue corresponding to the upward and downward directions, respectively. White colour indicates fully in-plane spin alignment. The tic values in parentheses in (d) refer to the pocket contours around the $\overline{K}$.

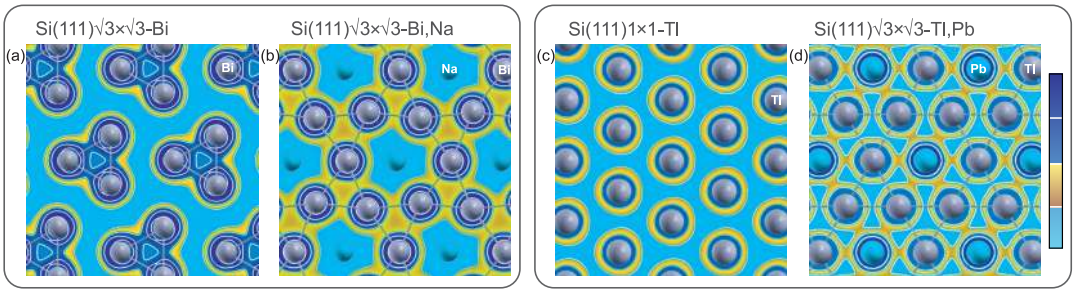

Figure 4 | Calculated electron density maps for (a) Bi/Si(111)$\sqrt{3}\times\sqrt{3}$, (b) (Bi, Na)/Si(111)$\sqrt{3}\times\sqrt{3}$, (c) Tl/Si(111)1 × 1, and (d) (Tl, Pb)$\Big/$Si(111) $\sqrt{3}\times\sqrt{3}$ surfaces. The multi-colour (blue-yellow) scale for electron density is used to highlight the interconnected electron density network at metallic alloy surfaces.

In particular, the (Bi, Na)/Si(111) band structure contains spin-split $\Sigma1$ ($\Sigma1'$) band which shows up in the Fermi map (Figure 3c and d) as two hexagon-shaped contours with corners pointing in the $\overline{\Gamma}-\overline{M}$ directions (where the splitting of the band is maximal, momentum splitting $\Delta k_{\|} = 0.044$ Å^{-1} and energy splitting $\Delta E_F =$ 210 meV). Besides, the $\Sigma1$ ($\Sigma1'$) band forms hole pockets having the shape of smoothed triangles around the $\overline{K}$ points. The out-of-plane spin component for pocket contours is negligible (albeit finite and different for neighboring pockets), the in-plane component dominates and the counterclockwise spin helicity is the same for all six pocket contours.

As for the (Tl, Pb)/Si(111), it displays the two spin-split metallic bands, $\Sigma1$ ($\Sigma1'$) and $\Sigma2$ ($\Sigma2'$). In the Fermi map of the $\Sigma1$ ($\Sigma1'$), the outer contour has almost round shape, while the inner contour is a hexagon with corners pointing in the $\overline{\Gamma}-\overline{K}$ directions. The maximal splitting for the $\Sigma1$ ($\Sigma1'$), $\Delta k_{\|} = 0.038$ Å^{-1} and $\Delta E_F = 250$ meV, is along $\overline{\Gamma}-\overline{M}$ direction. The other spin-split metallic band $\Sigma2$ ($\Sigma2'$) shows up as hexagonal contours with corners along the $\overline{\Gamma}-\overline{M}$ direction, i.e. rotated by 30° compared to the inner contour of the $\Sigma1$ band. The maximal splitting for the $\Sigma2$ ($\Sigma2'$), $\Delta k_{\|} = 0.050$ Å^{-1} and $\Delta E_F = 140$ meV, is along $\overline{\Gamma}-\overline{K}$ direction.

Comparing the Fermi contours of the present alloys with those found for spin-split surface states of the reported phases with hexagonal symmetry, one can notice certain common features. For example, the contour with two hexagons having corners in the $\overline{\Gamma}-\overline{M}$ directions (as for the (Bi, Na)/Si(111) $\Sigma1$ ($\Sigma1'$) and (Tl, Pb)/Si(111) $\Sigma2$ ($\Sigma2'$) bands) was also observed at the Pb/Ge(111)$\sqrt{3}\times\sqrt{3}$ surface[3]. The contour of (Tl, Pb)/Si(111) $\Sigma1$ ($\Sigma1'$) band with hexagon having corners in the $\overline{\Gamma}-\overline{K}$ directions inside a circle is akin that reported for Au/Si(111)$\sqrt{3}\times\sqrt{3}$[4] and Au/Ge(111)$\sqrt{3}\times\sqrt{3}$ [19].

Discussion

The shown examples of 2D alloying provide a hint for elucidating the pathways for converting the originally semiconducting surface into the metallic one. Note that both original surfaces, Bi/Si(111) $\sqrt{3}\times\sqrt{3}$ and Tl/Si(111)1 × 1, contain 1.0 ML of metal adsorbate. Taking into account that the surface lattice constant of Si(111) is 3.84 Å, such a density of adsorbate atoms is not sufficient to ensure the overlapping of their electron wave functions. This is clearly seen in the calculated electron density maps in Figure 4a and c: electron density is localized either around Bi trimers or single Tl atoms, respectively. Note that it is typical for metal-induced Si(111) reconstructions where the atomic layers with metallic properties develop usually at metal coverage beyond 1.0 ML (e.g., In/Si(111)$\sqrt{7}\times\sqrt{3}$ with 1.2 and 2.4 ML In[20] or Pb/Si(111)$\sqrt{3}\times\sqrt{3}$ with 1.33 ML Pb[21]). Another possibility is realized when the metal layer of 1.0 ML is compressed into the interconnected network due to Si atoms incorporated within the same reconstructed layer (e.g., Ag/Si(111)$\sqrt{3}\times\sqrt{3}$ [22,23] or Au/Si(111)$\sqrt{3}\times\sqrt{3}$ [24,25], each containing 1.0 ML metal and 1.0 ML Si). One can see that adding 1/3 ML Na to the Bi/Si(111)$\sqrt{3}\times\sqrt{3}$ produces a similar effect: Na adsorption causes originally isolated Bi trimers to rotate and grow in size until they form a chained-trimer structure. As a result, electron density associated with Bi atoms becomes arranged into the interconnected network (Figure 4b) responsible for appearance of the surface metallic properties. The (Tl, Pb)/Si(111) system looks seemingly similar, as originally isolated Tl atoms also form chained-trimer structure. However, the electron density map (Figure 4d) shows that actually the Tl-associated electron density is interconnected through that of the Pb atoms. Hence, appearance of the surface metallic properties is controlled here just by increasing metal-atom coverage at the surface.

Thus, our results demonstrate that formation of 2D alloys containing a metal with a strong spin-orbit coupling allows to obtain spin-split metallic surface-state bands on silicon. However, finding an appropriate metal pair is actually a challenging task. For example, while Na is a suitable component for making 2D alloy with Bi, it appears that the other alkali metals, Li and Cs, are not alloyed with Bi and grow as 3D islands on $\beta-$Bi/Si(111)$\sqrt{3}\times\sqrt{3}$ surface. Nevertheless, the list of the prospective alloys displaying variety of spin-related properties is believed to be very vast.

Methods

Sample preparation. The STM and ARPES experiments were performed in an ultra-high-vacuum Omicron MULTIPROBE system with a base pressure better than ~2.0 × 10^{-10} Torr. Atomically-clean Si(111)7 × 7 surfaces were prepared *in situ* by flashing to 1280°C after the samples were first outgassed at 600°C for several hours. Pristine Bi/Si(111)$\sqrt{3}\times\sqrt{3}$ and Tl/Si(111)1 × 1 reconstructions were formed by depositing 1 ML of the corresponding species onto Si(111)7 × 7 surface held at ~450°C and ~300°C, respectively. Sodium was deposited from a well-outgassed commercial SAES chromate dispenser, lead from a heated Pb-stuffed Mo tube.

STM. STM images were acquired using Omicron variable-temperature STM-XA operating in a constant-current mode. Electrochemically-etched W tips and mechanically cut PtIr tips were used as STM probes after annealing in vacuum.

ARPES. ARPES measurements were conducted in the ultrahigh vacuum chamber Omicron MULTIPROBE using VG Scienta R3000 electron analyzer and high-flux He discharge lamp ($h\nu = 21.2$ eV) with toroidal-grating monochromator as a light source.

Ab initio random structure search. Atomic structure of the new alloyed (Bi, Na)$\Big/$Si(111)$\sqrt{3}+\sqrt{3}$ and (Tl, Pb)$\Big/$Si(111)$\sqrt{3}\times\sqrt{3}$ reconstructions were elucidated using ab initio random structure search technique[26] after it had been successfully tested for the known Bi/Si(111)$\sqrt{3}\times\sqrt{3}$ and Tl/Si(111)1 × 1 structures.

First-principles calculations. Our calculations were based on DFT as implemented in the Vienna ab initio simulation package VASP[27,28], using a planewave basis and the projector-augmented wave approach[29] for describing the electron-ion interaction. The generalized gradient approximation (GGA) of Perdew, Burke, and Ernzerhof (PBE)[30] has been used for the exchange correlation (XC) potential. The Hamiltonian contains the scalar relativistic corrections, and the spin-orbit interaction (SOI) was taken into account by the second variation method as has been implemented in VASP by Kresse and Lebacq[31]. To simulate the reconstructions we use a slab consisting of 12 bilayers (BL). Hydrogen atoms were used to passivate the Si dangling bonds at the bottom of the slab. Both bulk Si lattice constant and the atomic positions within the

three BLs of the slab were optimized including SOI self-consistently. The silicon atoms of deeper layers were kept fixed at the bulk crystalline positions.

1. Rashba, E. Properties of semiconductors with an extremum loop. 1. Cyclotron and combinational resonance in a magnetic field perpendicular to the plane of the loop. *Sov. Phys. Solid. State* **2**, 1109–1022 (1960).
2. Bychkov, Y. & Rashba, E. Properties of a 2D electron gas with lifted spectral degeneracy. *JETP Letters* **39**, 78–81 (1984).
3. Yaji, K. *et al*. Large Rashba spin plitting of a metallic surface-state band on a semiconductor surface. *Nature Commun.* **1**, 17–5 (2010).
4. Bondarenko, L. V. *et al*. Large spin splitting of metallic surface-state bands at adsorbate-modified gold/silicon surfaces. *Sci. Rep.* **3**, 1826–6 (2013).
5. Gierz, I. *et al*. Silicon surface with giant spin splitting. *Phys. Rev. Lett.* **103**, 046803–4 (2009).
6. Sakamoto, K. *et al*. Peculiar Rashba splitting originating from the two-dimensional symmetry of the surface. *Phys. Rev. Lett.* **103**, 156801–4 (2009).
7. Frantzeskakis, E., Pons, S. & Grioni, M. Band structure scenario for the giant spin-orbit splitting observed at the Bi/Si(111) interface. *Phys. Rev. B* **82**, 085440–11 (2010).
8. Sakamoto, K. *et al*. Abrupt rotation of the Rashba spin to the direction perpendicular to the surface. *Phys. Rev. Lett.* **102**, 096805–4 (2009).
9. Ibañez-Azpiroz, J., Eiguren, A. & Bergara, A. Relativistic effects and fully spin-polarized Fermi surface at the Tl/Si(111) surface. *Phys. Rev. B* **84**, 125435–6 (2011).
10. Stolwijk, S. D., Schmidt, A. B., Donath, M., Sakamoto, K. & Krüger, P. Rotating spin and giant splitting: Unoccupied surface electronic structure of Tl/Si(111). *Phys. Rev. Lett.* **111**, 176402–5 (2013).
11. Zhu, X. G. *et al*. Observation of Rashba splitting on $\beta-\sqrt{3}\times\sqrt{3}$–Sb/Si(111) reconstructed surface. *Surf. Sci.* **618**, 115–119 (2013).
12. Park, J. *et al*. Self-assembled nanowires with giant Rashba split band. *Phys. Rev. Lett.* **110**, 036801–5 (2013).
13. Sakamoto, K. *et al*. Valley spin polarization by using the extraordinary Rashba effect on silicon. *Nature Commun.* **4**, 2073–6 (2013).
14. Miwa, R. H., Schmidt, T. M. & Srivastawa, G. P. Bi covered Si(111) surface revisited. *J. Phys.: Cond. Matt.* **15**, 2441–2447 (2003).
15. Lee, S. S. *et al*. Structural and electronic properties of thallium overlayers on the Si(111)-7 × 7 surface. *Phys. Rev. B* **66**, 233312–4 (2002).
16. Noda, T., Mizuno, S., Chung, J. & Tochihara, H. T_4 site adsorption of Tl atoms in a Si(111)-(1 × 1)-Tl structure, determined by low-energy electron diffraction analysis. *Jpn. J. Appl. Phys.* **42**, L319–L321 (2003).
17. Kim, N. D. *et al*. Structural properties of a thallium-induced Si(111)-1 × 1 surface. *Phys. Rev. B* **69**, 195311–5 (2004).
18. Kocán, P., Sobotík, P. & Ošťádal, I. Metallic-like thallium overlayer on a Si(111) surface. *Phys. Rev. B* **84**, 233304–4 (2011).
19. Höpfner *et al*. Three-dimensional spin rotations at the Fermi surface of a strongly spin-orbit coupled surface system. *Phys. Rev. Lett.* **108**, 186801–5 (2012).
20. Uchida, K. & Oshiyama, A. Identification of metallic phases of In atomic layers on Si(111) surfaces. *Phys. Rev. B* **87**, 165433–5 (2013).
21. Stepanovsky, S., Yakes, M., Yeh, V., Hupalo, M. & Tringides, M. C. The dense $\alpha-\sqrt{3}\times\sqrt{3}$Pb/Si(111) phase: A comprehensive STM and SPA-LEED study of ordering, phase transitions and interactions. *Surf. Sci.* **600**, 1417–1430 (2006).
22. Takahashi, T., Nakatani, S., Okamoto, N. & Ishikawa, T. A study of the Si(111)$\sqrt{3}\times\sqrt{3}-$Ag surface by transmission X-ray diffraction and X-ray diffraction topography. *Surf. Sci.* **242**, 54–58 (1991).
23. Katayama, M., Williams, R. S., Kato, M., Nomura, E. & Aono, M. Structure analysis of the Si(111)$\sqrt{3}\times\sqrt{3}R30-$Ag surface. *Phys. Rev. Lett.* **66**, 2762–2765 (1991).
24. Ding, Y. G., Chan, C. T. & Ho, K. M. Theoretical investigation of the structure of the $(\sqrt{3}\times\sqrt{3})R30-$Au/Si(111) surface. *Surf. Sci.* **275**, L691–L696 (1992).
25. Hong, I. H., Liao, D. K., Chou, Y. C., Wei, C. M. & Tong, S. Y. Direct observation of ordered trimers on Si(111)$\sqrt{3}\times\sqrt{3}$R30°$-$Au by scanned-energy glancing-angle Kikuchi electron wave-front reconstruction. *Phys. Rev. B* **54**, 4762–4765 (1996).
26. Pickard, C. J. & Needs, R. J. Ab initio random structure searching. *J. Phys.: Condens. Matter* **23**, 053201–23 (2011).
27. Kresse, G. & Hafner, J. Ab initio molecular dynamics for liquid metals. *Phys. Rev. B* **47**, 558–561 (1993).
28. Kresse, G. & Joubert, D. From ultrasoft pseudopotentials to the projector augmented-wave method. *Phys. Rev. B* **59**, 1758–1775 (1999).
29. Blöchl, P. E. Projector augmented-wave method. *Phys. Rev. B* **50**, 17953–17979 (1994).
30. Perdew, J. P., Burke, K. & Ernzerhof, M. Generalized gradient approximation made simple. *Phys. Rev. Lett.* **77**, 3865–3868 (1996).
31. Kresse, G., Marsman, M. & Furthmüller, J. VASP the Guide. http://cms.mpi.univie.ac.at/vasp/vasp/vasp.html, (2013) Date of access: 27/03/2014.

Acknowledgments

Part of this work was supported by the Russian Foundation for Basic Research (Grant Nos 12-02-00416, 13-02-00837, 13-02-12110, 14-02-31070) and the NSh-167.2014.2.

Author contributions

D.V.G., L.V.B. and A.V.M. carried out ARPES and STM under the support of A.A.Y. and A.Y.T.. J.P.C., C.M.W., S.V.E. and E.V.C. carried out the theoretical calculation. D.V.G., Y.L.W., A.V.Z. and A.A.S. analyzed the data and wrote the manuscript with input from J.P.C., M.Y.L., S.V.E. and E.V.C. and conceived and coordinated the project.

Additional information

Competing financial interests: The authors declare no competing financial interests.

How to cite this article: Gruznev, D.V. *et al*. A Strategy to Create Spin-Split Metallic Bands on Silicon Using a Dense Alloy Layer. *Sci. Rep.* **4**, 4742; DOI:10.1038/srep04742 (2014).